This document is downloaded from DR-NTU, Nanyang Technological University Library, Singapore.

Title	Material jetting additive manufacturing: An experimental study using designed metrological benchmarks
Author(s)	Yap, Yee Ling; Wang, Chengcheng; Sing, Swee Leong; Dikshit, Vishwesh; Yeong, Wai Yee; Wei, Jun
Citation	Yap, Y. L., Wang, C., Sing, S. L., Dikshit, V., Yeong, W. Y., & Wei, J. (2017). Material jetting additive manufacturing: An experimental study using designed metrological benchmarks. Precision Engineering, 50, 275 -285.
Date	2017
URL	http://hdl.handle.net/10220/44113
Rights	© 2017 Elsevier Inc. This is the author created version of a work that has been peer reviewed and accepted for publication by Precision Engineering, Elsevier Inc. It incorporates referee's comments but changes resulting from the publishing process, such as copyediting, structural formatting, may not be reflected in this document. The published version is available at: [http://dx.doi.org/10.1016/j.precisioneng.2017.05.015].

ACCEPTED MANUSCRIPT

Material jetting additive manufacturing: An experimental study using designed metrological benchmarks

Yee Ling Yap [a], (Y.L. Yap) ylyap@ntu.edu.sg

Chengcheng Wang [a], (C. Wang) wang1148@e.ntu.edu.sg

Swee Leong Sing [a], (S.L. Sing) sing0011@e.ntu.edu.sg

Vishwesh Dikshit [a], (V. Dikshit) vishdixit@ntu.edu.sg

Wai Yee Yeong [a], (W.Y. Yeong) wyyeong@ntu.edu.sg +65 6790 4343 (corresponding author)

Jun Wei [b], (J. Wei) jwei@simtech.a-star.edu.sg

Affiliations:

[a] Singapore Centre for 3D Printing, School of Mechanical & Aerospace Engineering, Nanyang Technological University

Address: 50 Nanyang Avenue, Singapore 639798

[b] Singapore Institute of Manufacturing Technology (SIMTech) @ NTU

Address: 73 Nanyang Drive, Singapore 637662

Highlights:

- Customized benchmarks were specifically designed to characterize and establish the process capability of material jetting AM technique
- Metrological studies were conducted to determine the effect of process parameters on dimensional accuracy of fabricated parts.
- Design limitations on special features such as thin walls and assembly-free parts fabricated using different build orientations were also evaluated.

ACCEPTED MANUSCRIPT

Abstract:

Additive manufacturing (AM) technique allows the creation of parts with a high degree of design complexity by building three-dimensional (3D) parts layer-by-layer. Many of the current restrictions of design for manufacturing (DFM) as well as design for assembly (DFA) are no longer applicable for AM due to the lack of needs for tooling. Instead, it is critical to establish the manufacturing limits and design guidelines to achieve optimal production outcomes. This can be achieved through manipulation of process parameters.

Keywords: Additive Manufacturing; 3D Printing; Metrology; Material Jetting; Inkjet Printing

The purpose of this paper is to establish a systematic methodology for investigating the process capability of the material jetting AM technique by using specially designed benchmark artifacts. In this study, three customized benchmarks were designed to characterize and establish the process capability of material jetting AM technique. Each of the benchmarks was designed for different purposes. Using a benchmark, metrological studies were conducted to determine the effect of process parameters on the dimensional accuracy of fabricated part. The design limitations on special features such as thin walls and assembly-free parts fabricated using different build orientations were also evaluated.

1. Introduction

Additive manufacturing (AM) technique allows the creation of parts with high design complexity as the three-dimensional (3D) parts are built layer-by-layer. With the advances of technology and material development, AM has been increasingly adopted for the creation of the end-use parts [1-6]. The manufacturing of end-use parts using AM could take advantage of the increased design freedom offered by AM to enhance the part functionality.

ACCEPTED MANUSCRIPT

Unlike traditional manufacturing technologies such as casting or molding, AM manufactures highly complex parts without the constraint of tooling. Many of the current restrictions of design for manufacturing (DFM) and design for assembly (DFA) are no longer applicable in the AM due to the elimination of tooling and part consolidation by merging of multiple parts [7, 8]. However, there are limited comprehensive design for additive manufacturing (DFAM) frameworks or guidelines established for parts with high geometrical complexity for the design engineers to take advantage of the expansive design freedom [9, 10]. Moreover, constraints in AM are typically process and material-dependent; different AM techniques cater to specific material groups and operate based on unique process mechanism. Hence, it is critical to study and establish the manufacturing and design guidelines for individual processes to achieve optimal production outcomes.

Vayre *et al.* [11, 12] and Hague *et al.* [13] obtained comprehensive information relating to manufacturing constraints of the AM processes then proposed design methodology or design guidelines for AM by analyzing the defined parameter sets. Through the understanding of manufacturing limitations, the manufacturing and design rules can be easily defined in order to achieve physical quality and geometrical accuracy [7]. Mellor *et al.* highlighted that in addition to the unique characteristics and constraints of AM, production planning and quality control are also influential factors to implement product design framework in AM [14]. Adam and Zimmer established the design rules by relating the manufacturability and quality of standard geometrical element to AM process settings [15]. This direct approach is also commonly used for comparing the dimensional accuracy and variation of the printed parts built by different AM techniques.

Material jetting additive manufacturing, or in particular, inkjet 3D printing technique is an established AM process that can create parts by depositing droplets of liquid photopolymers using

ACCEPTED MANUSCRIPT

piezo printing heads and curing the photopolymers using ultraviolet lamps. Inkjet 3D printers, such as PolyJet from Stratasys and MultiJet from 3D Systems, are capable of selectively depositing multiple photo-curable polymer resins simultaneously to fabricate multi-materials parts. Sacrificial support materials are automatically generated and deposited together with the photopolymers to support overhanging structures. The inkjet 3D printing technology has been widely adopted to produce not only prototypes but also functional polymer components such as lightweight honeycombs [16], lifestyle wearable products [1], custom anatomical models [4] as well as scaffolds for tissue engineering [17, 18]. Increasing adoption rate of the PolyJet inkjet printing technology to produce functional products thus motivates many researchers in the field of material properties characterization [19-21], dimensional and geometrical characterization [22, 23] as well as new application like 4D printing [6, 24, 25] and multi-material reinforced structures [26, 27].

In inkjet 3D printing, printing orientation is one of the critical process parameters to determine the dimensional accuracy, surface quality, and strength property. However, the orientation that minimizes materials and building time is more commonly used while neglecting these effects [19]. The effects of the process parameters, such as part position, printing orientation, nozzle cleanliness and machine preparation can be systematically investigated by establishing design of experiments (DoE) [20, 28]. DoE can be extended to analyze the process parameters for the optimal geometrical quality.

Besides looking at the process parameters, the quality and the types of features are also important in order to develop the manufacturing and design guidelines. A number of researchers identified such needs to quantify the quality of the 3D printed parts, in terms of dimensional accuracy and surface quality. Using the NAS 979 test part, which was developed in 1966 as a test part for computer numerically controlled (CNC) machining to evaluate CNC machine performance, Cook

ACCEPTED MANUSCRIPT

and Soons investigated the geometric errors of AM parts. Since it was designed for CNC machining instead of AM, it could not highlight the errors of AM systems and explore the accuracy of small features [29]. Most of the benchmarking studies used specially designed artifacts to measure and evaluate the geometrical quality and accuracy of the printed parts [30-34] and the performance of an AM machine or process, in terms of manufacturing speed and efficiency [30, 33].

Benchmark parts can be designed accordingly to evaluate manufacturing and design capabilities of different AM systems in fabricating different geometric features, for examples, holes and bosses in rectangular, round, spherical, conical and L-shaped, ramps, overhangs, freeform structures, side notches and angles [35, 36]. The benchmark artifact developed by National Institute of Standards and Technology (NIST) in an effort to propose a standard test artifact for AM, has incorporated most of the aforementioned features to test the capability of different machines or processes [37]. Some studies also established the correlation between the geometrical designs and the corresponding Geometric Dimensioning and Tolerancing (GD&T) characteristics, for example, straightness, flatness, circularity, cylindricity, perpendicularity, angularity, parallelism, symmetry, and concentricity [36-38]. Nevertheless, geometric tolerancing remains challenging in AM due to several AM process-driven specification issues such as build direction and location, layer thickness, and support structures, to tolerancing the complex free-form surfaces, topology-optimized features and internal features [39]. In addition, there are needs for benchmark parts to be designed specifically for the intended application. For example, Lee *et al.* have designed a benchmark specifically for microfluidic chip application to evaluate the printing resolution, accuracy, repeatability of PolyJet and FDM [40]. Seepersad *et al.* also designed several benchmark artifacts to study the limiting sizes for features such as slits, mating gears, and shafts for moving

ACCEPTED MANUSCRIPT

mechanical components produced in a single build using selective laser sintering (SLS) process [41]. With specifically designed benchmarks, the information will be useful for designers and production engineers, to create first-time-right design and fabrication, while optimizing production yield.

In this study, specially designed benchmark parts were used, with the objective to achieve optimal part quality and to metrologically quantify the manufacturing constraints of material jetting AM technique, also known as inkjet 3D printing. This study utilizes customized benchmark designs to characterize and to highlight the process and manufacturing capability of the inkjet AM technique, for various purposes. First, optimal process parameters, including layer thickness, building location, and surface finishing type that could affect the dimensional accuracy of the printed parts, were evaluated. By using specially designed benchmarks with various specific features, manufacturing and design considerations for building thin walls as well as assembly-free parts along different orientations were also derived.

2. Benchmarks Design and Experimental Details

2.1 Optimal Process Parameters

A simple benchmark part has been designed in the size of 30 x 30 x 30 mm for characterizing the part's dimensional accuracy, as shown in Fig. 1. The length, width and height of the printed part also correspond to the printing accuracy with respect to its X-, Y- and Z-axes. The benchmark parts in this study were manufactured by Objet500 Connex3 PolyJet printer (Stratasys, MN, USA) using VeroWhite Plus (RGD835) material.

The effects of PolyJet process parameters on the surface roughness and the building time as well as materials consumptions of the finals parts have been investigated [30, 42, 43]. However, few

ACCEPTED MANUSCRIPT

have attempted to determine the influence on the dimensional accuracy of the printed parts. Using the benchmark, the effects of PolyJet process parameters on the part accuracy, particularly in terms of length, width and height of the PolyJet printed part was investigated.

The three process parameters that are considered in this study include (A) layer thickness, (B) surface finishing type and (C) building location. Factorial experiment was adopted to fully investigate the effects of each parameter. In this study, three input parameters accompanied with two levels are summarized in Table 1.

The length, width and height of the printed part have been chosen as the main process response characteristics to investigate the influence of the process parameters. The three dimensions (length, width and height) were measured using a coordinate measuring machine (CMM) Werth Video-Check-IP (Werth Messtechnik GmbH, Giessen, Germany). The resolution of the CMM is 0.5 µm and its accuracy is $1.5 + L/500$ µm (where L is the measuring length). Non-contact optical method utilizing 5X vision optics was used to measure the specimens. The average temperature at the time of measurement was maintained at 20 ^{o}C. Six repetitions of measurements were taken and averaged to obtain the mean result.

For three parameters at two levels, a full factorial design requires 2^3 or eight experiments. The factorial experimental design is shown in Table 2. Each run was repeated three times with the same conditions to minimize random errors. The experiment is classified into a Nominal-the-best (NB) design because the closest nominal values for the three dimensions including length, width and height, are the most desired in this case.

ANOVA was performed to determine significant differences among the three factors by calculating the F-ratio and their significance. Based on the ANOVA, the relative importance of the

ACCEPTED MANUSCRIPT

process parameters with respect to the dimensional accuracy was investigated to determine the optimal PolyJet processing parameters. The ANOVA was carried out for the confidence level of 99 %. The normality of the data was tested using the Anderson-Darling method and this was analysed using Minitab 17 (Minitab, Inc, USA). The length, width and height have *p*-values of 0.479, 0.27 and 0.077, respectively, which are larger than the alpha level of 0.01. The normal probability plots of the residuals shown in Fig. 2 also approximately follow a straight line, indicating that the residuals of the data follow a normal distribution.

2.2 Manufacturing Constraints for Thin Walls

PolyJet is capable of fabricating fine features owing to its ability to deposit tiny liquid droplets in high resolution of 600 dpi in both the X- and Y-axes, and 1600 dpi in the Z-axis, with minimum layer thickness of 16 μm [44]. For lightweight purpose, it has been demonstrated that fully solid structures can be replaced by building thin shells while strengthening the internal structure by filling honeycomb structures [2, 45]. Hence, it is necessary to identify the PolyJet manufacturing constraints in building thin walls so that the intended thin-walled structure like honeycomb can be built effectively.

The benchmark design for thin wall application should be able to characterize the dimensional accuracy in terms of length, width and height of the PolyJet built parts in various orientations. The benchmark parts were measured using the coordinate measuring machine with non-contact optical method, with 5X objective magnification. All features on the same benchmark part are independent of one another. The same benchmark design, shown in Fig. 3, was fabricated with nine different wall thicknesses, including 0.20 mm, 0.30 mm, 0.40 mm, 0.50 mm, 0.60 mm, 0.70 mm, 0.80 mm, 0.90 mm and 1.00 mm. Each part consists of 13 thin walls oriented at different angles ranging from 0 degree to 180 degrees, with respect to the y-axis of PolyJet building direction, with an

ACCEPTED MANUSCRIPT

increment of 15 degrees. The angle increases in the clockwise direction, as shown in Fig. 3. Every thin wall consists of a staircase made up of 4 varying heights of 5mm, 10mm, 15mm and 20mm.

The benchmark part was manufactured by Objet500 Connex3 using VeroWhitePlus RGD835 rigid opaque material at layer thickness of 32 µm. Glossy surface finish setting was selected for printing the parts. The dimensions were measured using optical CMM with 5X objective lens. The heights were measured and calculated by taking the distance between the datum plane which is the top of the base plate of the benchmark, to the top planes of each thin walls. The plane was taken as an average from at least 4 positions at each height. The thickness measurements were also repeated 3 times for every thickness at every height over 3 random positions.

2.3 Lowest Clearance Limits for Assembly-free Parts

AM can build working assemblies as a single component, eliminating the need to assemble various components for a functional product. The specified clearance between two moving components are dependent on the AM process limitations, including the layer thickness and the powder or droplet size, and the post-cleaning process that includes the ability to remove support material or support structures that are formed in between the moving components [39]. In this study, two benchmark parts aiming to investigate the minimum clearance between the most typical mating parts, including sliding slots, shaft and holes, and adjacent cubes along different axes, were designed, as shown in Fig. 4.

Hole-based system is adopted for shaft and hole features; the size of the hole is kept constant while the shaft size is varied to obtain different fits. Benchmark A was designed such that the cube features are attached on a baseplate which has a size of 124.0 x 73.6 x 14.0 mm. On the other hand, the cubes were designed and printed without baseplate in the benchmark B, allowing the cubes to

ACCEPTED MANUSCRIPT

be separated when they are not fused together. The shafts, cylinders and cubes were positioned 1mm higher than the base plane of Benchmark A so that the parts can be detached from the baseplate, after removing the support material. The purpose and dimensions of each feature in the benchmark parts are listed in Table 3.

3. Results and Discussions

3.1 Optimal Process Parameters

The measurement results for the mean and standard uncertainty of length, width and height measurement results are presented in Table 4.

Table 5 shows the results of the ANOVA analysis for the length, width and height. For F distribution, the probability of type I error is 1%, which gives 99% confidence in the ANOVA analysis. It can be deduced that surface finish type is the most significant process parameter that affects the accuracy of the length. There are no significant parameters that affect the accuracy of the width. Building location is the most significant process parameter that affects the height accuracy. The effects of the two significant process parameters (factor B and factor C) on the mean length and height are shown in Fig. 5. On the other hand, the interaction effects were found to be insignificant for the length, width and height.

Factor B (surface finish type) is more significant for printing in the x-axis. In principle, matte finish option offers a better part accuracy [28]. This is because every surface of the part is coated with support materials to preserve its original geometry. Factor C (location of building) is the significant factor for printing in the z-axis. Factor C at level 1, which is the top-left position, produces the part with height lower than its nominal value, while the part has a larger than its nominal height at level 2 (bottom-right). The reason why building parts in top-left position has a negative deviation might

ACCEPTED MANUSCRIPT

be due to the non-uniform UV light exposure on the build tray. The print head always moves back to the home position in the x-axis before moving to the y-axis, leading to a higher UV exposure near the origin of x [28]. The parts in top-left might be over-cured by the UV light, and shrinkage of the part, as compared to the parts printed in the bottom-right of the build tray.

The dimensional accuracy of length, width and height of the PolyJet printed also represents the printing accuracy of PolyJet with respect to different printing axis, as shown in Table 4. The dimension of the parts printed along the z-axis is the most accurate, followed by the x-axis and y-axis. This finding agrees with Lee et al.'s results [40]. It is also observed that the height of the parts printed is more accurate than the width and length [46]. One possible reason is that the stepper motor can precisely control the height of the build tray and the levelling roller can wipe off the extra amount of the material droplets, maintaining consistent height increment for every layer.

3.2 Manufacturing Constraints of Thin Walls

The deviations of the height from its corresponding nominal value for wall thickness smaller than 0.4 mm and larger than 0.4 mm are shown in Fig. 6 and Fig. 7 respectively. It is observed that the thin walls with wall thickness smaller than 0.4 mm tend to have relatively larger and negative deviation from its corresponding nominal value, implying that they cannot be built to the intended height regardless of the building orientation and built height. Walls thinner than 0.5 mm are also more likely to be skewed and not perpendicular to the base due to compressive forces and rolling motion of the roller and wiper in the levelling system. For walls thicker than 0.4 mm, the height deviations for walls oriented from 45 degrees to 135 degrees, are noticeably larger than the other angles. Thin walls at these angles are more likely to have height deviated more than 0.200 mm. However, the deviation is not pronounced for other walls that have larger than 0.4 mm width. Despite the high resolution of the machine, which should deposit layer of resins as small as 16 μm,

ACCEPTED MANUSCRIPT

the deviation in height for PolyJet printing in the glossy mode for parts thicker than 0.4 mm is typically ± 0.200 mm. It can be concluded that in order to build the thinnest wall with higher consistency and accuracy in height without defects, using the PolyJet, the wall thickness must be larger than 0.4 mm.

The percentage deviation of wall thickness from nominal value at various orientations is summarized in Table 6. The tip thickness was measured directly from the tip of each walls while the mean thickness was calculated from the thickness measured at the mid and near the base of the walls. The tip thickness is typically smaller than the mean thickness as the height increases and the edges are rounded as shown in Fig. 8. This is likely due to the spreading of the build material before being cured by the UV light and this also explains the thickness at the base is larger than that at the tip. Moreover, the thickness deviation becomes greater as the orientation angle increases. Thin walls oriented at 90° have the largest deviation from its respective nominal wall thickness. The reason is attributed to the thin wall built is parallel to the moving direction of the print head and the leveling roller, which is embedded and travels along with the printing head. The extra amount of material droplets might be wiped off the wall, resulting in the large deviation and hence dimensional inaccuracy when printing at 90°.

3.3 Lowest Clearance Limits for Assembly-free Parts

Benchmarks were fabricated at HS mode which prints at a layer thickness of 32 µm, using VeroClear RGD810 transparent material. The benchmark parts were positioned at the top-left of the build tray. Two sets of benchmarks were fabricated using “glossy” and “matte” surface finishing option. The benchmark parts with “glossy” surface finishing before removing the support material are shown in Fig. 9(a) and Fig. 9(b). Support materials were removed after post-processing, and parts including the shafts, cylinders and cubes, which did not fuse during printing

ACCEPTED MANUSCRIPT

were detached to demonstrate the limits and fits of these features, as shown in Fig. 9(c) and Fig. 9(d).

The features that did not fuse together are considered to be resolvable, and therefore can be removed from the baseplate or be separated from each other, after removing the support material using high-pressure water jet. Based on this principle, the minimum clearance can be characterized. The cube X and cube Y, as shown in Fig. 9(b) and 9(d) respectively, in benchmark A are resolvable if the gap between two parts are clearly visible and there are no signs of fusion. On the other hand, the determination of minimum clearance in the shafts and holes feature as well as sliding slot feature depends on whether the cylinders are separable. The minimum clearance characterization results printed in glossy and matte finishing are presented in Table 7 and Table 8, respectively. The benchmark result shows that the minimum clearances that must be specified in between the shafts and holes under glossy and matte finishing are 0.4 mm and 0.2 mm, respectively. For other features printed in glossy mode, the minimum clearance required in the y-axis are consistent at 0.3 mm. However, the clearance required between the sliding slots and the cylinders in the x-axis is noticeably smaller (0.2 mm) than that for the cube features (0.4 mm for cubes with the baseplate and 0.5 mm for cubes without baseplate). The results for benchmark printed in matte mode show that the minimum clearances for both cubes with and without baseplate in the X- and Y-axes are consistent at 0.15mm. On the other hand, the cylinder and sliding slots require a minimum clearance of 0.1 mm and 0.2 mm, in the X- and Y-axes, respectively.

The result shows that minimum clearance gap for parts printed in matte finish is generally smaller as compared to that in glossy finish. This finding, however, does not conform to the result for dimensional accuracy as discusses previously. The accuracy of the parts printed in glossy mode is better than in the matte finishing, however, the extra support materials that are selectively

ACCEPTED MANUSCRIPT

deposited around the parts in the matte finishing play a significant role in creating the clearance gap. Printing in glossy mode without additional support material filling up the fine gaps and coating around the model material would lead to agglomeration of the excess resin swept by the wiper at the base causing the neighbouring parts to fuse when the clearance gap is too small, as illustrated in Fig. 10. On the other hand, as the parts are enveloped with support material when printing in matte mode, as shown in Fig. 11, the agglomeration of the nearby photopolymer droplets and thus fusion of two neighbouring parts could be prevented. The likelihood for the photopolymers droplet to spread upon dropping on the build tray is also lowered when printing in matte surface finish mode, thus prohibiting separate components to fuse after UV photopolymerization. The clearance gaps shown in the result also show the minimum gap required to remove the support material effectively using water jet.

These results can be useful when printing parts with moving components like a joint or a hinge. Printing in matte mode produces a significantly more consistent result for such parts and multiple components that are placed close to one another.

5. Conclusions

In this paper, optimal PolyJet printing process parameters were obtained. Printing with matte surface finish mode and printing along z-axis produce better dimensional accuracy. Furthermore, the effects of printing orientation on the dimensional accuracy of thin walls were investigated. The result shows that the wall thickness must be greater than 0.4 mm to ensure that thin walls can be built successfully. It is also recommended to orientate thin walls 0 ° along the y-direction for the best accuracy in width and height. Lastly, minimum clearances for mating features were also characterized. The recommendation for printing parts that are closed to one another or mating features is the use of matte surface finish mode.

ACCEPTED MANUSCRIPT

This study provides a systematic methodology to study the manufacturing and design capability of the PolyJet 3D printing process. Through this study, the importance of benchmark designs, incorporating targeted features and metrology, to allow unconstrained characterization or measurement in AM parts is highlighted. Current study focuses on small features that are in the milli-scale, nonetheless, these benchmark designs can be readily scaled for further investigations in both smaller and larger scales.

Acknowledgement

This project is funded under A*STAR TSRP - Industrial Additive Manufacturing Programme by A*STAR Science & Engineering Research Council (SERC) (Work Package 4).

References

[1] Yap YL, Lai YM, Zhou HF, Yeong WY. Compressive strength of thin-walled cellular core by inkjet-based additive manufacturing. In: Chua CK, Yee YW, Jen TM, Erjia L, editors. Proceedings of the 1st International Conference on Progress in Additive Manufacturing. Singapore2014. p. 333-8.

[2] Yap YL, Yeong WY. Shape recovery effect of 3D printed polymeric honeycomb. Virtual and Physical Prototyping. 2015;10:91-9.

[3] Sing SL, An J, Yeong WY, Wiria FE. Laser and electron-beam powder-bed additive manufacturing of metallic implants: A review on processes, materials and designs. Journal of Orthopaedic Research. 2016;34:369-85.

[4] Yap YL, Tan YSE, Tan HKJ, Peh ZK, Low XY, Yeong WY, et al. 3D printed bio-models for medical applications. Rapid Prototyping Journal. 2016;23.

ACCEPTED MANUSCRIPT

[5] Sun Z, Tan X, Tor SB, Yeong WY. Selective laser melting of stainless steel 316L with low porosity and high build rates. Materials & Design. 2016;104:197-204.

[6] Khoo ZX, Teoh JEM, Liu Y, Chua CK, Yang S, An J, et al. 3D printing of smart materials: A review on recent progresses in 4D printing. Virtual and Physical Prototyping. 2015;10:103-22.

[7] Ponche R, Kerbrat O, Mognol P, Hascoet J-Y. A novel methodology of design for Additive Manufacturing applied to Additive Laser Manufacturing process. Robotics and Computer-Integrated Manufacturing. 2014;30:389-98.

[8] Liu J. Guidelines for AM part consolidation. Virtual and Physical Prototyping. 2016;11:133-41.

[9] Kumke M, Watschke H, Vietor T. A new methodological framework for design for additive manufacturing. Virtual and Physical Prototyping. 2016;11:3-19.

[10] Cooper DE, Stanford M, Kibble KA, Gibbons GJ. Additive Manufacturing for product improvement at Red Bull Technology. Materials & Design. 2012;41:226-30.

[11] Vayre B, Vignat F, Villeneuve F. Designing for Additive Manufacturing. Procedia CIRP. 2012;3:632-7.

[12] Vayre B, Vignat F, Villeneuve F. Identification on some design key parameters for additive manufacturing: Application on electron beam melting. Procedia CIRP. 2013;7:264-9.

[13] Hague R, Mansour S, Saleh N. Material and design considerations for rapid manufacturing. International Journal of Production Research. 2004;42:4691-708.

[14] Mellor S, Hao L, Zhang D. Additive manufacturing: A framework for implementation. International Journal of Production Economics. 2014;149:194-201.

[15] Adam GAO, Zimmer D. Design for Additive Manufacturing—Element transitions and aggregated structures. CIRP Journal of Manufacturing Science and Technology. 2014;7:20-8.

ACCEPTED MANUSCRIPT

[16] Dikshit V, Nagalingam PA, Yap LY, Sing LS, Yeong YW, Wei J. Investigation of Quasi-Static Indentation Response of Inkjet Printed Sandwich Structures under Various Indenter Geometries. Materials. 2017;10.

[17] Yeong WY, Chua CK, Leong KF, Chandrasekaran M, Lee M-W. Development of scaffolds for tissue engineering using a 3D inkjet model maker. Virtual Modelling and Rapid Manufacturing: Advanced Research in Virtual and Rapid Prototyping Proc 2nd Int Conf on Advanced Research in Virtual and Rapid Pro. 2005:115-8.

[18] Chua CK, Yeong WY, Leong KF. Rapid prototyping in tissue engineering: a state-of-the-art report. Virtual Modeling and Rapid Manufacturing. 2005:19-27.

[19] Cazón A, Morer P, Matey L. PolyJet technology for product prototyping: Tensile strength and surface roughness properties. Proceedings of the Institution of Mechanical Engineers, Part B: Journal of Engineering Manufacture. 2014;228:1664-75.

[20] Barclift MW, Williams CB. Examining variability in the mechanical properties of parts manufactured via polyjet direct 3d printing. International Solid Freeform Fabrication Symposium. Austin, TX, USA2012.

[21] Blanco D, Fernandez P, Noriega A. Nonisotropic experimental characterization of the relaxation modulus for PolyJet manufactured parts. Journal of Materials Research. 2014;29:1876-82.

[22] Ibrahim D, Broilo TL, Heitz C, de Oliveira MG, de Oliveira HW, Nobre SM, et al. Dimensional error of selective laser sintering, three-dimensional printing and PolyJet models in the reproduction of mandibular anatomy. Journal of cranio-maxillo-facial surgery : official publication of the European Association for Cranio-Maxillo-Facial Surgery. 2009;37:167-73.

ACCEPTED MANUSCRIPT

[23] Meisel N, Williams C. An Investigation of Key Design for Additive Manufacturing Constraints in Multimaterial Three-Dimensional Printing. Journal of Mechanical Design. 2015;137:111406-.

[24] Tibbits S. 4D Printing: Multi-Material Shape Change. Architectural Design. 2014;84:116-21.

[25] Yu K, Ritchie A, Mao Y, Dunn ML, Qi HJ. Controlled Sequential Shape Changing Components by 3D Printing of Shape Memory Polymer Multimaterials. Procedia IUTAM. 2015;12:193-203.

[26] Sugavaneswaran M, Arumaikkannu G. Analytical and experimental investigation on elastic modulus of reinforced additive manufactured structure. Materials & Design. 2015;66:29-36.

[27] Brooks H, Molony S. Design and evaluation of additively manufactured parts with three dimensional continuous fibre reinforcement. Materials & Design. 2016;90:276-83.

[28] Mueller J, Shea K, Daraio C. Mechanical properties of parts fabricated with inkjet 3D printing through efficient experimental design. Materials & Design. 2015;86:902-12.

[29] Cooke AL, Soons JA. Variability in the geometric accuracy of additively manufactured test parts. The Twenty-First Annual International Solid Freeform Fabrication (SFF) Symposium – An Additive Manufacturing Conference. Austin, Texas, USA2010. p. 1-12.

[30] Oh YT, Kim GD. A benchmark study on rapid prototyping processes and machines: quantitative comparisons of mechanical properties, accuracy, roughness, speed, and material cost. Proceedings of the Institution of Mechanical Engineers, Part B: Journal of Engineering Manufacture. 2008;222:201-15.

[31] Ippolito R, Iuliano L, Gatto A. Benchmarking of rapid prototyping techniques in terms of dimensional accuracy and surface finish. CIRP Annals - Manufacturing Technology. 1995;44:157-60.

ACCEPTED MANUSCRIPT

[32] Yang HY, Lim JC, Liu YC, Qi XY, Yap YL, Dikshit V, et al. Performance evaluation of ProJet multi-material jetting 3D printer. Virtual and Physical Prototyping. 2017;12:95-103.

[33] Kruth J, Vandenbroucke B, Vaerenbergh J, Merceli P. Benchmarking of different sls/slm processes as rapid manufacturing techniques. International Conference Polymers & Moulds Innovations. Gent, Belgium2005.

[34] Cavallini B, Ciurana J, Reguant C, Delgado J. Studying the repeatability in DMLS technology using a complete geometry test part. Innovative Developments in Design and Manufacturing: CRC Press, 2009.

[35] Fahad M, Hopkinson N. A new benchmarking part for evaluating the accuracy and repeatability of Additive Manufacturing (AM) processes. 2nd International Conference on Mechanical, Production and Automobile Engineering (ICMPAE 2012). Singapore2012. p. pp. 28-9.

[36] Mahesh M, Wong YS, Fuh JYH, Loh HT. Benchmarking for comparative evaluation of RP systems and processes. Rapid Prototyping Journal. 2004;10:123-35.

[37] Moylan S, Slotwinski J, Cooke A, Jurrens K, Donmez MA. Proposal for a standardized test artifact for additive manufacturing machines and processes. Proceedings of the Solid Freeform Fabrication Symposium. 2012:902-20.

[38] Yang L, Anam MA. An investigation of standard test part design for additive manufacturing. Proceedings of the Solid Freeform Fabrication Symposium. 2014:901-22.

[39] Ameta G, Lipman R, Moylan S, Witherell P. Investigating the Role of Geometric Dimensioning and Tolerancing in Additive Manufacturing. Journal of Mechanical Design. 2015;137:111401--10.

ACCEPTED MANUSCRIPT

[40] Lee JM, Zhang M, Yeong WY. Characterization and evaluation of 3D printed microfluidic chip for cell processing. Microfluidics and Nanofluidics. 2016;20:1-15.

[41] Seepersad CC, Govett T, Kim K, Lundin M, Pinero D. A Designer's Guide for Dimensioning and Tolerancing SLS parts. p. 921-31.

[42] Udroiu R, Mihail LA. Experimental determination of surface roughness of parts obtained by rapid prototyping. Proceedings of the 8th WSEAS International Conference on Circuits, systems, electronics, control & signal processing. Puerto De La Cruz, Tenerife, Canary Islands, Spain: World Scientific and Engineering Academy and Society (WSEAS), 2009. p. 283-6.

[43] Kumar K, Kumar GS. An experimental and theoretical investigation of surface roughness of poly-jet printed parts. Virtual & Physical Prototyping. 2015;10:23-34.

[44] Objet350 and Objet500 Connex3. 2016.

[45] Yap YL, Lai YM, Zhou H, Yeong WY. Compressive strength of thin-walled cellular core by inkjet-based additive manufacturing. Proceedings of 1st International Conference on Progress in Additive Manufacturing. 2014:333-8.

[46] Meisel NA. Design for Additive Manufacturing Considerations for Self-Actuating Compliant Mechanisms Created via Multi-Material PolyJet 3D Printing. 2015.

Figure Caption

ACCEPTED MANUSCRIPT

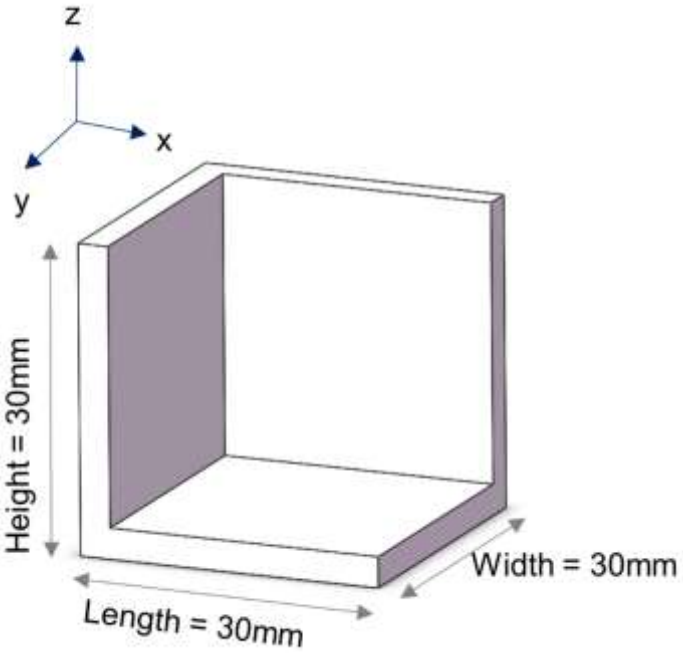

Figr-1

ACCEPTED MANUSCRIPT

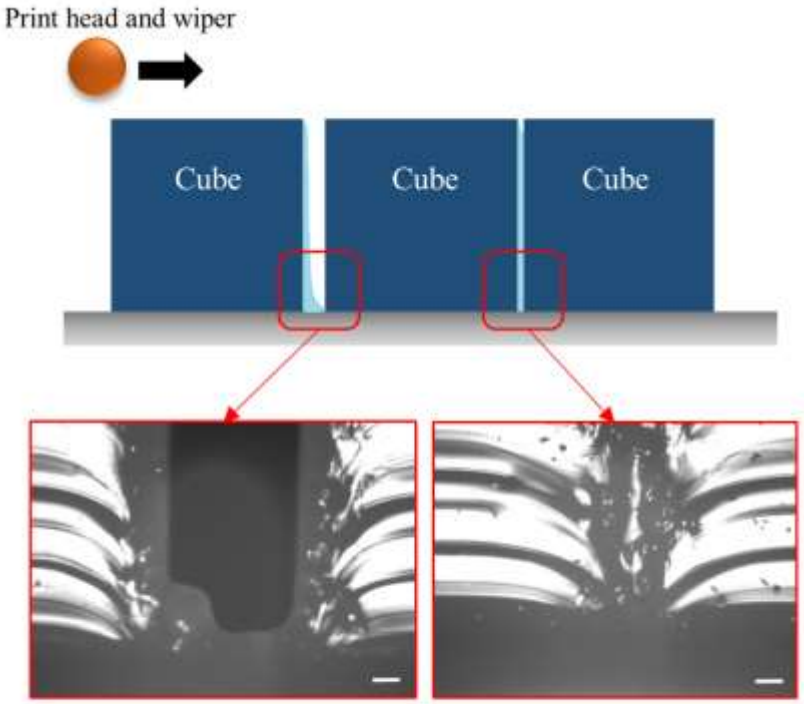

Excess resin being swept by the wiper agglomerating at the base

The agglomerated resin fuses with the neighbouring parts when the gap is too small

Figr-2

ACCEPTED MANUSCRIPT

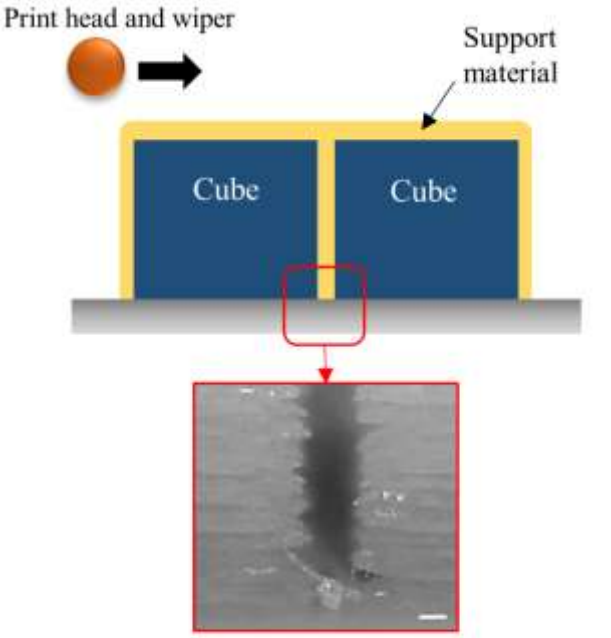

Support material is removed, leaving clear gap without agglomeration of resin

Figr-3

ACCEPTED MANUSCRIPT

Figr-4

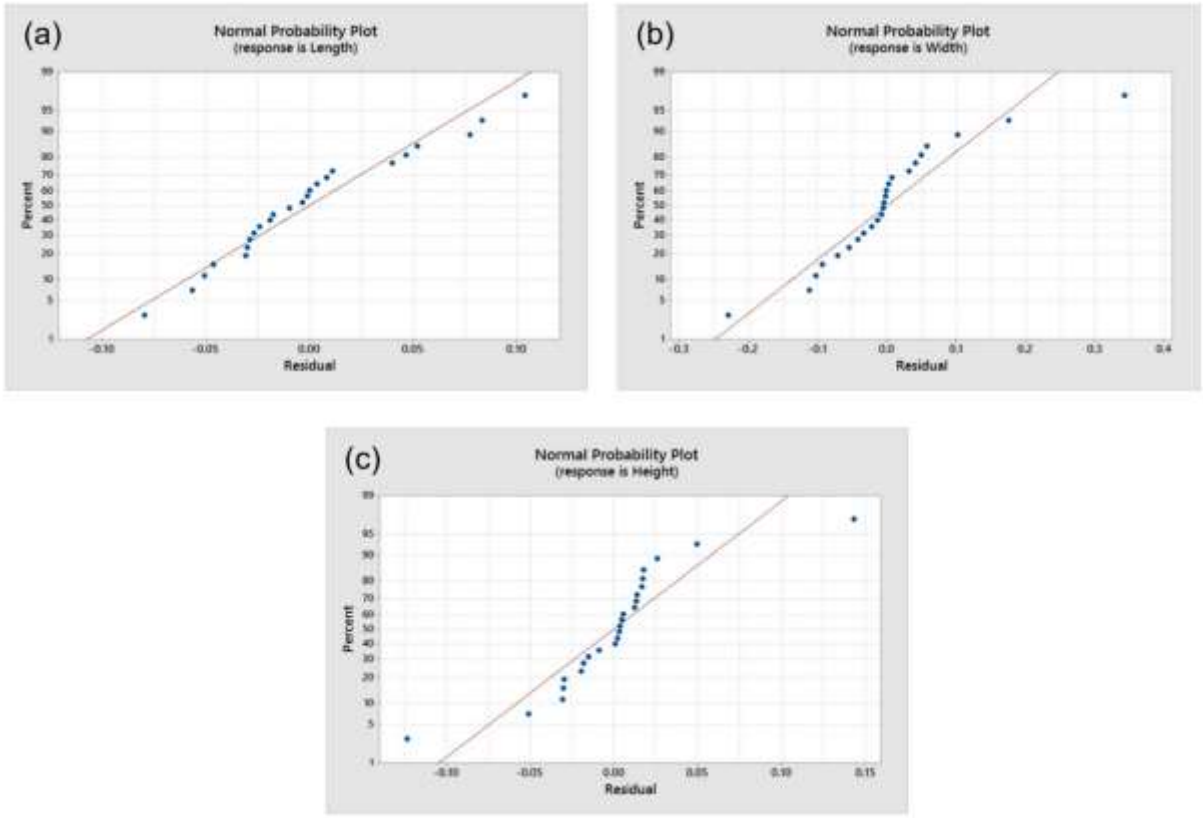

ACCEPTED MANUSCRIPT

Figr-5

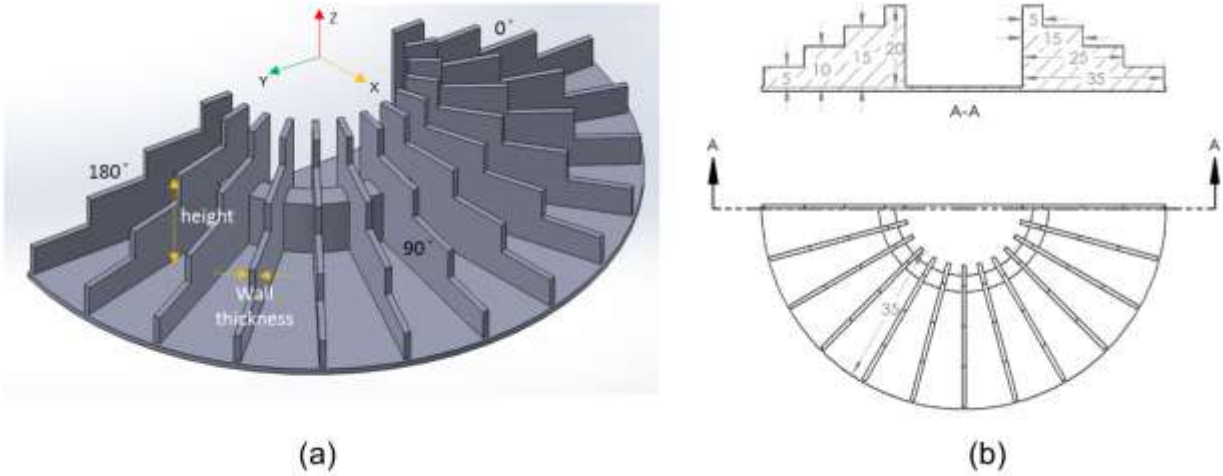

(a) (b)

ACCEPTED MANUSCRIPT

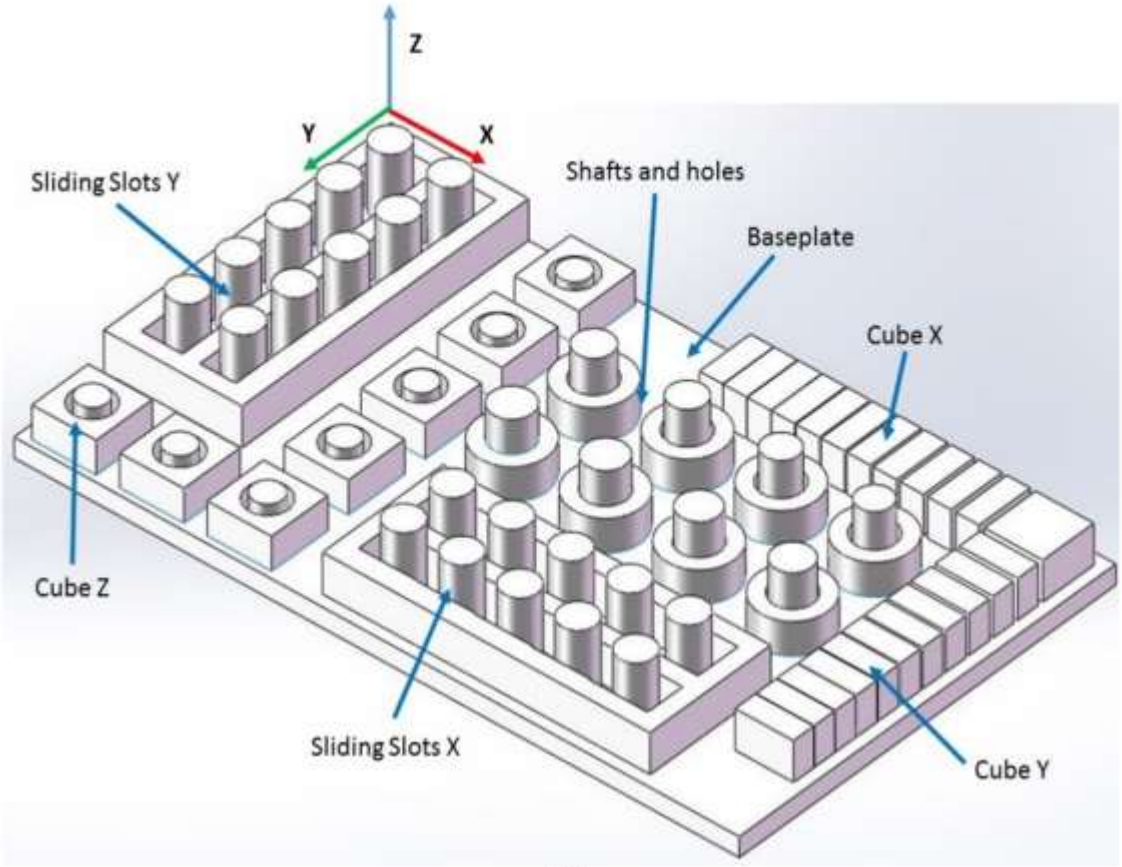

(a)

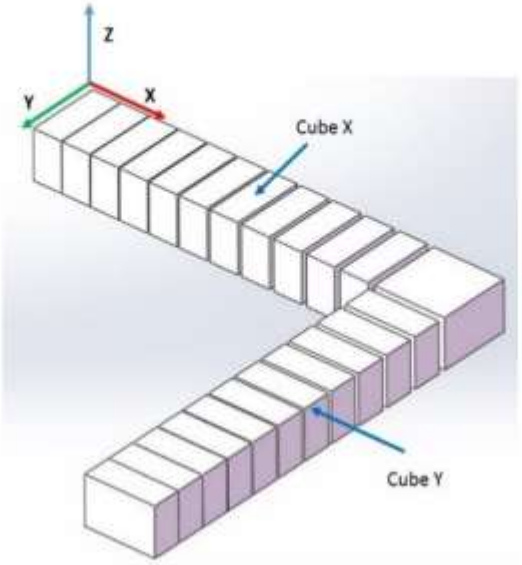

(b)

Figr-6

ACCEPTED MANUSCRIPT

Figr-7

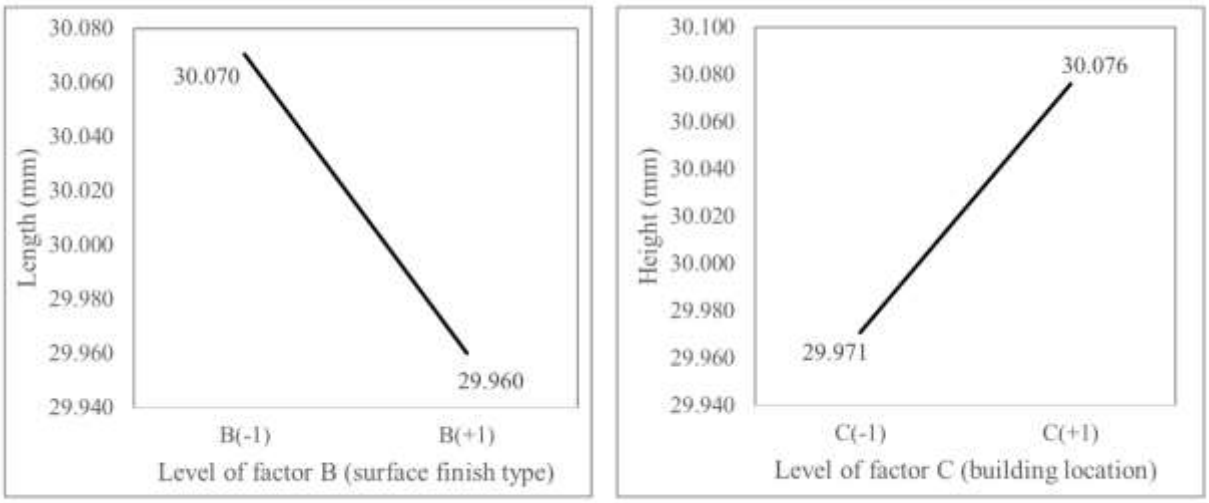

(a) (b)

ACCEPTED MANUSCRIPT

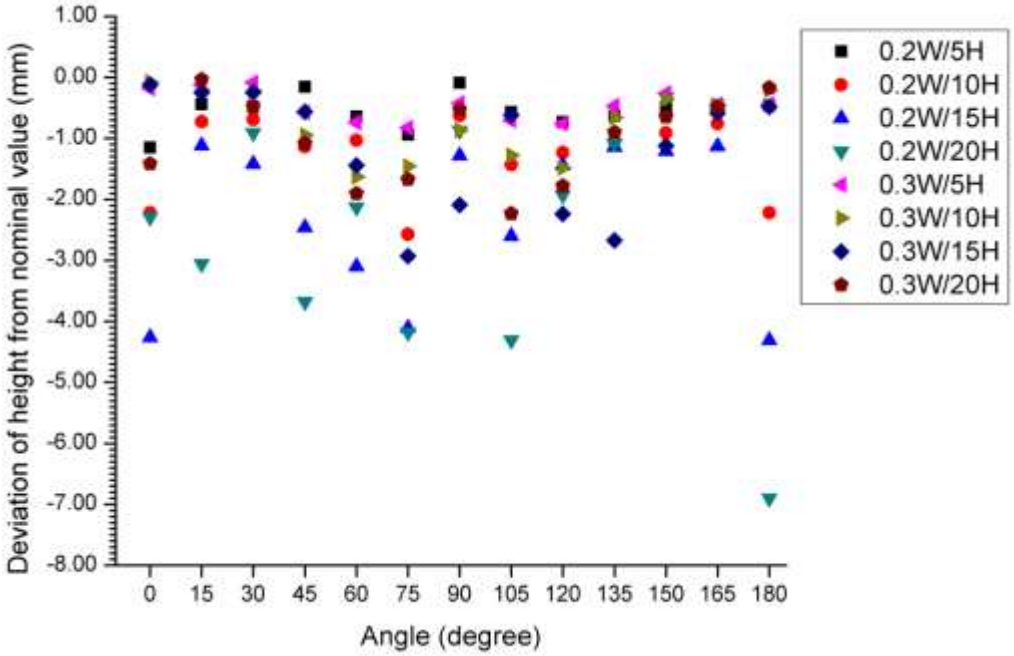

Figr-8

ACCEPTED MANUSCRIPT

Figr-9

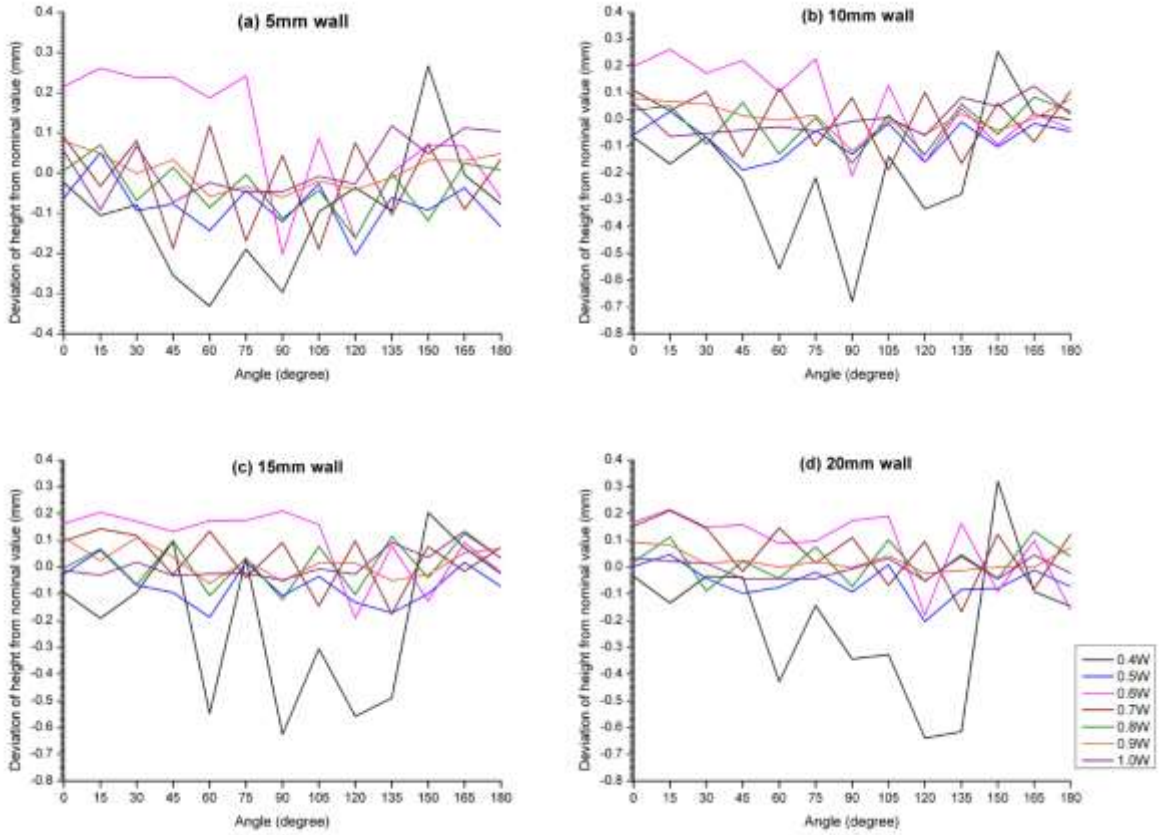

ACCEPTED MANUSCRIPT

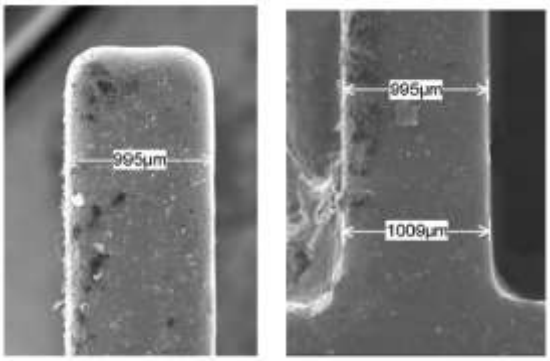

(a) (b)

Figr-10

ACCEPTED MANUSCRIPT

Figr-11

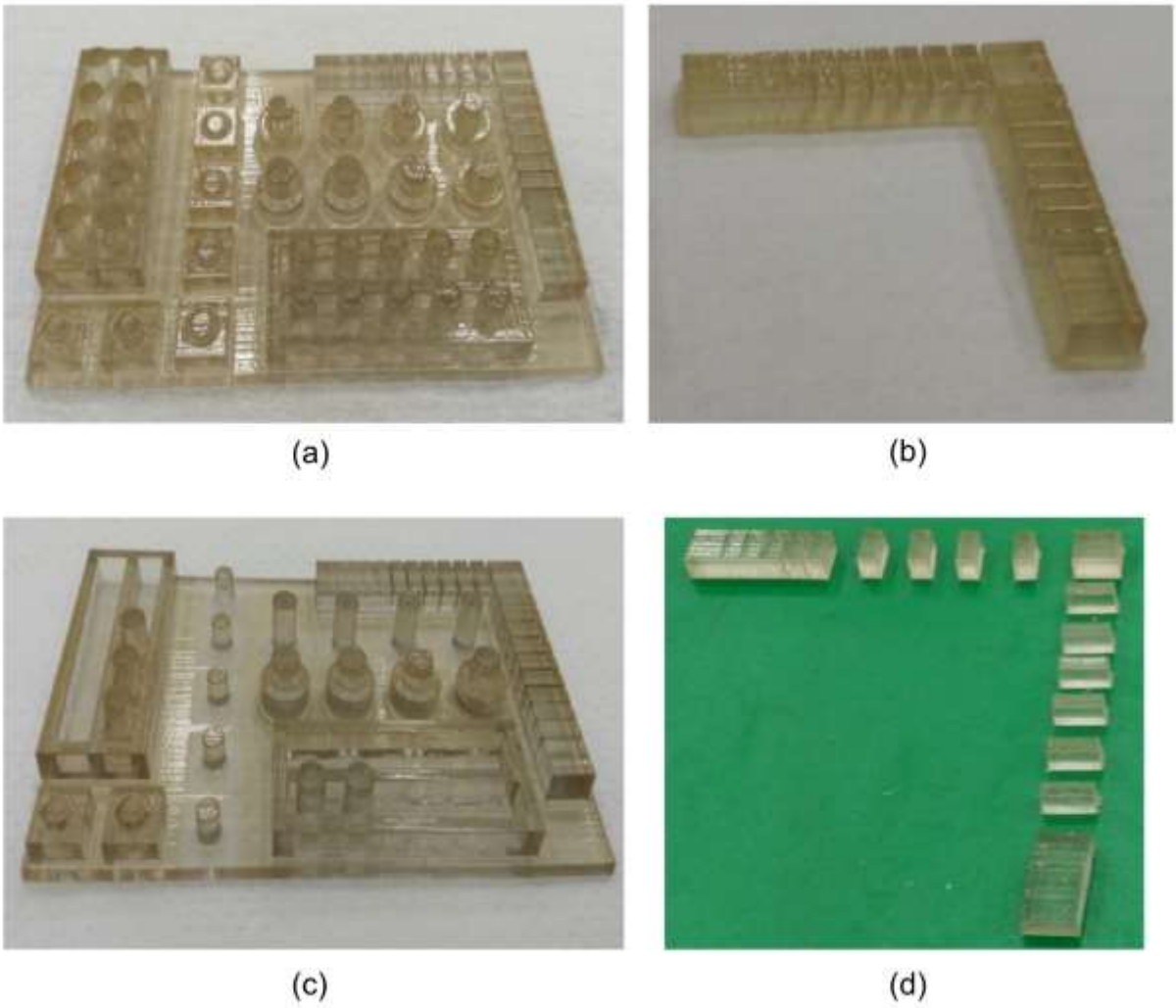

ACCEPTED MANUSCRIPT

Figr-12**Figure Captions**

Fig. 1. Benchmark part design for dimensional accuracy of length, width and height.

Fig. 2. Normal probability plot of the residuals for (a) length, (b) width, and (c) height

Fig. 3. (a) PolyJet 3D printed benchmark part designed to characterize the wall thickness (b) dimensions of the height and width for the thin walls (Unit: mm).

Fig. 4. Benchmark A and (b) benchmark B for minimum clearance between mating parts The cylinders in the sliding slot features are kept constant and only the gap between the sliding slot and the cylinder is varied between 0.05 mm to 0.9 mm.

Fig. 5. The effects of process parameters on the mean length and height: (a) factor B, (b) factor C.

Fig. 6. Deviation of height from nominal height for wall thickness < 0.4mm (W denotes wall thickness width and H denotes the wall height).

ACCEPTED MANUSCRIPT

Fig. 7. Deviation of height from nominal height for wall thickness ≥ 0.4mm at height of (a) 5mm, (b) 10mm, (c) 15mm and (d) 20mm.

Fig. 8. (a) Rounded edges at the tip of the 1.0 mm thin wall, (b) base of the 1.0 mm thin wall

Fig. 9. (a) Benchmark A before post processing, (b) benchmark B before post processing, (c) benchmark A after post-processing with unfused parts detached and (d) benchmark B after post-processing.

Fig. 10. Schematic and microscope images showing the agglomeration of the resin and fusion of two neighboring parts when printing in glossy mode. (Scale: 0.1mm)

Fig. 11. Schematics and microscope image showing the agglomeration of the resin and fusion of two neighboring parts when printing in glossy mode. (Scale: 0.1mm)

ACCEPTED MANUSCRIPT

Table 1

Experimental factors for part accuracy.

Quality Characteristics:	**Length, width and height of the part**	
Target Value	30 mm	
Control Factors	Level 1	Level 2
A. Layer Thickness	16 μm	32 μm
B. Surface Finish Type	Glossy	Matte
C. Location of Building	Top-left	Bottom-right

Table 2

2^3 full factorial design

Experimental Run Number	**Run**	**A**	**B**	**C**	**AB**	**AC**	**BC**	**ABC**
1	(1)	-	-	-	+	+	+	-
2	a	+	-	-	-	-	+	+
3	b	-	+	-	-	+	-	+
4	ab	+	+	-	+	-	-	-
5	c	-	-	+	+	-	-	+
6	ac	+	-	+	-	+	-	-
7	bc	-	+	+	-	-	+	-
8	abc	+	+	+	+	+	+	+

ACCEPTED MANUSCRIPT

Table 3

Interpretation for clearance of different features

Feature	Purpose	Part dimension	Clearance between two adjacent parts (mm)
Shafts and Holes	Shaft and hole assembly	Inner diameter of bore: 7mm	0.05, 0.1, 0.2, 0.3, 0.4, 0.5, 0.6, 0.7
Sliding Slots X and Y	Sliding joints	Diameter of solid cylinder: 6 mm	0.05, 0.1, 0.2, 0.3, 0.4, 0.5, 0.6, 0.7, 0.8, 0.9
Cube X and Y	Resolvable gap between cubes	N.A.	0.05, 0.1, 0.2, 0.3, 0.4, 0.5, 0.6, 0.7, 0.8, 0.9, 1.0
Cube Z	Separating the cube from the baseplate	N.A.	0.02, 0.05, 0.1, 0.2, 0.3, 0.4, 0.5

ACCEPTED MANUSCRIPT

Table 4

Experiment run number	Measurement results		
	Length (mm)	Width (mmm)	Height (mm)
1	30.038 ± 0.023	29.953 ± 0.027	29.987 ± 0.004
2	30.099 ± 0.043	30.215 ± 0.057	29.954 ± 0.008
3	29.871 ± 0.021	29.998 ± 0.083	29.983 ± 0.029
4	30.011 ± 0.054	30.104 ± 0.004	29.943 ± 0.015
5	30.080 ± 0.039	30.132 ± 0.032	30.107 ± 0.016
6	30.064 ± 0.002	30.168 ± 0.024	29.993 ± 0.015
7	29.941 ± 0.030	30.120 ± 0.174	30.036 ± 0.010
8	30.017 ± 0.010	29.918 ± 0.025	30.068 ± 0.078
Mean	30.015	30.076	30.009
Standard Uncertainty	0.044	0.062	0.033

Measurement results for length, width and height (mean ± standard uncertainty, 3 repetitions)

ACCEPTED MANUSCRIPT

Table 5

ANOVA analysis for (a) length, (b) width, and (c) height in mm

Factors	SS	DOF	MS	F_0	$F_{0.01,v1,v2}$	Significance
(a) Length						
A	0.025422	1	0.025422	8.224131	8.53	NO
B	0.072831	1	0.072831	23.56163	8.53	YES
C	0.002569	1	0.002569	0.831056	8.53	NO
AB	0.010918	1	0.010918	3.532214	8.53	NO
AC	0.007551	1	0.007551	2.442778	8.53	NO
BC	0.001746	1	0.001746	0.564823	8.53	NO
ABC	6.11E-05	1	6.11E-05	0.019773	8.53	NO
Error	0.049457	16	0.003091			
Total	0.170555	23				
(b) Width						
A	0.015211	1	0.015211	0.933069	8.53	NO
B	0.04041	1	0.04041	2.478838	8.53	NO
C	0.001734	1	0.001734	0.106368	8.53	NO
AB	0.058135	1	0.058135	3.566145	8.53	NO
AC	0.107575	1	0.107575	6.598964	8.53	NO
BC	0.014435	1	0.014435	0.885508	8.53	NO
ABC	0.002526	1	0.002526	0.154927	8.53	NO
Error	0.260829	16	0.016302			
Total	0.500855	23				
(c) Height						
A	0.009029	1.000000	0.009029	3.096197	8.53	NO
B	0.000045	1.000000	0.000045	0.015466	8.53	NO
C	0.042529	1.000000	0.042529	14.584445	8.53	YES
AB	0.007042	1.000000	0.007042	2.414817	8.53	NO
AC	0.000040	1.000000	0.000040	0.013643	8.53	NO
BC	0.000127	1.000000	0.000127	0.043696	8.53	NO
ABC	0.008775	1.000000	0.008775	3.009022	8.53	NO
Error	0.046657	16.000000	0.002916			
Total	0.114244	23				

ACCEPTED MANUSCRIPT

Table 6

Percentage deviation of wall thickness from nominal value

Nominal value (mm)	Deviation percentage (%) of wall thickness													
	0°		15°		30°		45°		60°		75°		90°	
	Tip	Mean	Tip	Mean	Tip	Mean	Tip	Mean	Tip	Mean	Tip	Mean	Tip	Mean
0.2	55.6	64.2	23.5	55.0	24.4	60.8	31.9	69.2	35.9	80.8	42.0	105.0	32.1	118.3
0.3	-1.6	12.8	0.1	27.8	2.5	28.9	12.5	30.6	6.6	36.1	14.7	46.1	23.8	40.0
0.4	0.7	12.9	-1.5	15.8	7.0	17.1	2.3	22.5	1.9	26.7	7.0	37.5	-0.9	39.2
0.5	-5.1	3.7	-6.7	7.3	-5.3	9.7	-0.9	11.7	-2.5	14.0	1.7	17.3	-0.2	20.0
0.6	-8.3	3.9	-6.2	3.6	-5.1	6.1	-4.2	5.8	-4.0	11.4	0.2	15.8	2.9	20.0
0.7	-12.0	3.1	-7.8	4.0	-6.5	5.7	-4.6	7.9	-5.4	8.3	-1.5	14.5	-8.1	20.0
0.8	-7.3	0.4	-7.7	2.3	-5.5	5.2	-3.5	6.3	-3.7	7.3	-0.5	13.0	6.6	15.0
0.9	-8.4	-0.9	-7.0	3.5	-7.7	4.3	-5.3	5.9	-5.1	8.1	-0.4	9.8	-4.8	14.4
1	-4.8	-1.7	-6.1	2.2	-5.0	4.7	-5.0	6.0	-1.9	7.7	0.1	8.8	-9.6	11.3

ACCEPTED MANUSCRIPT

Table 7

Minimum clearance for benchmark printed in glossy finishing

Feature	Minimum clearance in X-axis	Minimum clearance in Y-axis	Minimum clearance in Z-axis
Shafts and Holes		0.4 mm	
Sliding Slots	0.2 mm	0.3 mm	N.A.
Cubes attached to baseplate	0.4 mm	0.3 mm	N.A.
Cubes without baseplate	0.5 mm	0.3 mm	0.1 mm

Table 8

Minimum clearance for benchmark printed in matte finishing.

Feature	Minimum clearance in X-axis	Minimum clearance in Y-axis	Minimum clearance in Z-axis
Shafts and Holes		0.2 mm	
Sliding Slots	0.1 mm	0.2 mm	N.A.
Cubes attached to baseplate	0.15 mm	0.15 mm	N.A.
Cubes without baseplate	0.15 mm	0.15 mm	0.1 mm